Fresh and Aged Organic Aerosol Emissions from Renewable Diesel-Like Fuels HVO and RME in a Heavy-Duty Compression Ignition Engine

Novakovic, Maja; Eriksson, Axel; Gren, Louise; Malmborg, Vilhelm; Shamun, Sam; Karjalainen, Panu; Svenningsson, Birgitta; Tunér, Martin; Verhelst, Sebastian; Pagels, Joakim

Published in:
Technical paper - WCX SAE World Congress Experience

DOI:
10.4271/2023-01-0392

2023

Document Version:
Peer reviewed version (aka post-print)

23PFL-0663

Fresh and Aged Organic Aerosol Emissions from Renewable Diesel-Like Fuels HVO and RME in a Heavy-Duty Compression Ignition Engine

Author, co-author (Do NOT enter this information. It will be pulled from participant tab in MyTechZone)

Affiliation (Do NOT enter this information. It will be pulled from participant tab in MyTechZone)

Abstract

A modern diesel engine is a reliable and efficient mean of producing power. A way to reduce harmful exhaust and greenhouse gas (GHG) emissions and secure the sources of energy is to develop technology for an efficient diesel engine operation independent of fossil fuels. Renewable diesel fuels are compatible with diesel engines without any major modifications. Rapeseed oil methyl esters (RME) and other fatty acid methyl esters (FAME) are commonly used in low level blends with diesel. Lately, hydrotreated vegetable oil (HVO) produced from vegetable oil and waste fat has found its way into the automotive market, being approved for use in diesel engines by several leading vehicle manufacturers, either in its pure form or in a mixture with the fossil diesel to improve the overall environmental footprint. There is a lack of data on how renewable fuels change the semi-volatile organic fraction of exhaust emissions. In order to characterize and explain the difference in exhaust emissions from fossil diesel, HVO and RME fuels, particulate matter (PM) emissions were sampled at two exhaust positions of an experimental single cylinder Scania D13 heavy-duty (HD) diesel engine: at the exhaust manifold, and after a diesel oxidation catalyst (DOC). Advanced analyzing techniques were used to characterize the composition of the organic PM. Special attention was paid to an operating point at 18% intake oxygen level with constant engine operating conditions where the emission level of nitrogen oxides (NOx) was low, and carbon monoxide (CO) and total hydrocarbon (THC) were relatively low. On-line aerosol mass spectrometry (AMS) suggests that the chemical composition of the organic aerosols (OAs) was similar for HVO and diesel. However, RME both reduced the OA emissions and changed the composition with evidence for fuel signatures in the mass spectra. When the emissions were aged in an oxidation flow reactor to simulate secondary organic aerosol (SOA) formation in the atmosphere, it was found that OA concentration strongly increased for all fuels. However, SOA formation was substantially lower for RME compared to the other fuels. The DOC strongly reduced primary organic emissions in both the gas (THC) and particle phase (OA) and only marginally affected OA composition. The DOC was also effective in reducing secondary organic aerosol formation upon atmospheric aging.

Introduction

Aerosol particles in the atmosphere have adverse effects on air quality. The smallest size particles easily penetrate the human pulmonary system and have been linked to severe short- and long-term health impacts, such as asthma, cardiopulmonary diseases, and lung cancer [1]. Since some aerosols mainly scatter solar radiation back into space and thereby cool the climate, while others, like BC, contribute to warming, they present one of the largest uncertainties in climate modelling and prediction. They also affect the climate indirectly through their role as cloud condensation nuclei (CCN) and ice-nuclei [2].

Primary particles in vehicle exhaust, called particulate matter (PM) include soot particles with mean particle diameter around 30–100 nm [3][4] and nucleation mode particles, commonly with a solid core, usually below 10–15 nm [5]. Undiluted vehicle exhaust emissions in the tailpipe contain also a variety of different gaseous components, mainly volatile organic compounds (VOCs) and sulfuric acid, which get diluted and cool down [6][7][8]. The aerosol precursors, both organic and inorganic compounds, that were in gaseous phase at the tailpipe (due to the high exhaust gas temperatures) may nucleate to form new nucleation mode particles or they may condense on other particles (e.g. non-volatile core or accumulation mode) [9]. Thus, the fresh exhaust aerosol comprises the solid particles in the tailpipe (primary PM) and the newly formed particles during the seconds of mixing of the exhaust gas with ambient air [10][11]. Which process dominates, condensation or nucleation, depends on the availability of pre-existing particle surface area (condensation sink) [12] along with the dilution and cooling rate [13].

A large fraction (~50%) of the submicron aerosol particle mass in the troposphere is a complex mixture of hundreds of different organic compounds [14][15]. Organic aerosol (OAs) can be classified as either primary organic aerosol (POA) directly emitted by different sources, including anthropogenic (transportation and combustion activities) and biogenic, or secondary organic aerosol (SOA) formed upon chemical reactions in the atmosphere.

Secondary PM from combustion engines consists mainly of organic compounds and ammonium nitrate [16][17]. SOA is produced via secondary formation in the atmosphere, i.e. atmospheric aging, after the oxidation of gas-phase VOCs or hydrocarbon precursors [18][19], including polycyclic aromatic hydrocarbons (PAHs) [20]. The emissions of secondary PM precursors depend on fuel properties as well as engine type, load and aftertreatment system [21][22][23][16]. Both fuel and lubrication oil are significant sources of hydrocarbons emitted from diesel engines [24][25][26][27], however lubrication oil has been proposed to dominate POA emissions [28][29] and have stronger influence on the SOA formation than the fuel composition [16][17][23][30].

This process is complicated since each VOC can undergo a number of atmospheric degradation processes to produce a range of oxidized products, which may or may not contribute to SOA formation and growth [18]. There is also a difference between processes controlling particle number and processes controlling particle mass; condensation of vapors (sulfuric and nitric acids, ammonia, and secondary organics) onto existing particles may dominate particle mass without necessarily influencing particle number [31].

Recent studies have shown that the total OA caused by vehicles might be mostly down to SOA [17]. A better understanding of semi-volatile compounds from vehicles is needed in order to estimate their contribution to secondary aerosol formation [9]. Also, in order to make more accurate climate models, the behavior of aerosols in the atmosphere needs to be better understood [32]. Statistical analyses of the mass spectral data have a strong potential to provide detailed information on the sources and components of organic aerosol [33][34]. To interpret the results of these statistical methods, however, mass spectral signatures of various organic aerosol sources and components are needed [33]. The source appointment of OA measured in the air can distinguish factors with specific temporal variation and mass spectral patterns [19].

The O:C ratio of the POA and SOA material is a parameter that is expected to be closely related to an organic molecule's polarity and hydrophilicity, which are important parameters that influence particle properties such as the phase behavior [35][36] or SOA formation during approximately a week-long atmospheric residence period [37][38]. The O:C ratio has the practical advantage that it can be readily measured for atmospheric POA and SOA using online aerosol mass spectrometry [39].

The main factors influencing PM toxicity include chemical composition (e.g. the organic fraction), surface area, and the place of deposition in the respiratory tract upon inhalation. The deposited fraction primarily depends on the size, but also shape and density of the aerosol particles [40]. According to the size of the largest aerodynamic diameter in the group, PM can be classified as coarse (PM_{10}), fine ($PM_{2.5}$), submicron (PM_1) and ultrafine ($PM_{0.1}$). PM_{10} are mostly deposited in the upper airways, where they stay until removed by clearance mechanisms [40]. $PM_{2.5}$ can also penetrate deep into the respiratory tract, reaching the lungs, and due to their large surface areas, they can carry toxic material [41]. $PM_{0.1}$ are, however, deposited in the alveolar region of lungs that have only weak nanoparticle elimination mechanisms. They may translocate beyond the lung and cause adverse effects on the central nervous system, extrapulmonary organs and cause dysfunction of blood vessels causing negative cardiac effects [42][43].

Direct injection compression ignition (DICI) diesel fuelled internal combustion engines (ICEs) are renowned for their high efficiency, durability and high torque output, and therefore are an important propulsion technology for heavy-duty (HD) transport. They have a potential to keep the important place in the transition to sustainable HD transportation. The drawback of a DICI engine is that it is emitting harmful exhaust and affecting the climate, particularly if using fossil fuels. The negative impact of transportation can be reduced if fossil diesel fuel is exchanged for a diesel-like fuel of non-fossil origin. The use of 100% renewable diesel can achieve comparable lifecycle greenhouse gas (GHG) reduction to the use of electric vehicles (EVs), allowing for faster decarbonization of existing fleets in the short term [44].

Fatty acid methyl ester (FAME) fuels, often called *biodiesel*, can be produced from primary vegetable oils such as soy, palm, coconut, or sunflower oil, etc, and therefore belong to first-generation biofuels made from edible biomass. Rapeseed oil methyl ester (RME) is made by esterification of rapeseed oil by use of methanol, possibly biomethanol in the future. In Europe, most vehicles with DICI engines currently use low level blends of FAME in diesel, known as B5 or B7. Blending of increasing fractions of oxygen-containing FAME biodiesel fuels, produced from renewable biomass resources, into fossil diesel is currently encouraged to mitigate GHG emissions [45][46]. In order to study the effects of the directives, it is important to characterize emission signatures from biodiesel. The advantages of RME combustion are significantly reduced emissions of unburned hydrocarbon (HC), carbon monoxide (CO) and particulate matter [47]. However, pure RME can produce slightly higher NOx emissions if used as a drop-in fuel, i.e. without changing the original diesel engine settings. NOx can actually go down, too [48]. RME can have detrimental effects on fuel injection systems [49]. Also, RME has higher density and lower energy content than diesel, as well as poor cold flow properties [50] and oxidation stability. Furthermore, the quality of FAME is dependent on the properties of the feedstock used, thus limiting the choice of feedstock suitable for cold climate regions [51].

On the other hand, high levels of hydrotreated vegetable oil (HVO) fuel can be blended with fossil diesel without affecting the engine performance. HVO can also be used neat and is then commonly called *renewable diesel*. Fuel properties of HVO are close to fossil diesel fuel and therefore, their logistics, storage, and combustion properties are similar [51][52]. The HVO production process involves removal of oxygen from the triglycerides by the use of hydrogen. Moreover, the HVO properties are not as sensitive to different feedstocks of vegetable oil as in the case of biodiesel. Edible oils are the main feedstock for HVO production, but non-edible oils, such as pongamia, can also be used for its production, as well as used frying oil, fat residues from the meat and fish industry, and technical corn oil (a residue from ethanol production) and then it can be classified as a second-generation biofuel.

Third-generation biofuels, based on feedstocks such as micro algae and microbes, have recently come into research focus in the field of fuel production [53], and research on more affordable fourth-generation biofuels based on genetically modified algae is following [54]. Until completely sustainable and renewable biofuels get developed for future use in ICEs, currently available HVO and FAME-type fuels can significantly reduce PM, HC, and CO emissions in diesel exhaust [55][56] and change the particle size distribution and soot nanostructure [47][57] in comparison to fossil diesel fuel.

Switching to these renewable and sustainable fuels has shown the potential to reduce GHG emissions [58] and improve the air quality with the existing fleets of vehicles, especially of those without an exhaust aftertreatment system (EATS) [21]. EATSs are designed to reduce multiple pollutants found in diesel exhaust [59]. The main function of a diesel oxidation catalyst (DOC) is to ensure the sufficient oxidation of the gas phase HC and CO, but also to remove the condensable organic fraction while still in the gas phase [60][61]. It also significantly decreases the secondary aerosol formation of both diesel and HVO [23], as well as for RME [21]. However, there is still little to no knowledge on the effects on the emitted organic aerosol composition and its sources (fuel, lube oil, combustion generated).

Throughout this study, Swedish MK1 ultra-low sulfur fossil diesel and two renewable diesel fuels, HVO and RME, were used without blending. The first part of the paper is focused on the study of the engine behaviour under fixed operating conditions, linking it to the fuel used. In the main part, PM is analysed without and with use of a DOC. The focus is on the analysis of the chemical composition of the OA, as well as SOA after the experimental simulation of atmospheric aging of emissions using an oxidation flow reactor. Emission signatures from the three different fuels and at different stages of the EATS are investigated.

Specifically, this paper aims to give answers to the following questions:

- How do RME and HVO affect OA and SOA chemical composition?
- What effect does the DOC have on OA and SOA composition?

- What is the elemental composition of the OA (H:C and O:C ratio)? Is there evidence for fuel specific signature in the mass spectra?
- How does this relate to oxygen introduced by the fuel, by oxidation during combustion and oxidation in the DOC?

Method

Experimental setup

Engine and operation

The engine used in this experiment was a Scania D13 six-cylinder HD DICI engine with one active and five deactivated cylinders, operating at a steady state low load of 6 bar gross indicated mean effective pressure (IMEP). Heavy-duty engines operating over low load duty cycles are typical for urban environments that require large quantities of goods and services for commercial and domestic use such as refuse pickup [62].

Figure 1 shows the schematic diagram of the experimental engine and surrounding setup. The existing equipment was used and therefore the engine piston was of the standard stepped bowl shape with geometrical r_c of 17.3:1. Table 1 lists the specifications of the experimental engine.

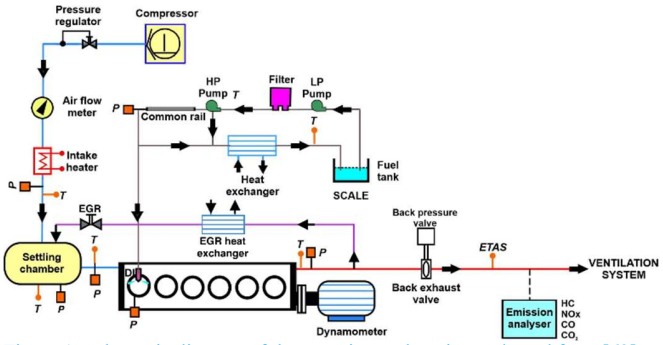

Figure 1. Schematic diagram of the experimental engine. Adapted from [63] with permission.

Table 1. Specifications of the experimental engine

Cylinders	originally six, operated on one (cylinder 6)
Displacement volume	2124 [cm^3]
Stroke	160 [mm]
Bore	130 [mm]
Connecting rod length	255 [mm]
Geometrical r_c	17.3:1
Number of valves	4

The fuel was injected at a rail pressure of 1200 bar through an injector with 10 holes and 148° umbrella angle connected to a common rail and a high-pressure injection (XPI) fuel pump. The combustion phasing was kept constant throughout the experiment with CA50 at ~5 crank angle degrees after top dead center (CAD ATDC).

The engine was connected to an electric motor rotating at a constant 1200 rpm. It motored the engine during the start-up and switch-off phases, and kept the engine at a constant rotational speed when fired. A water cooled Kistler pressure transducer measured the relative in-cylinder pressure. The data used in this study were collected from the engine and averaged over 300 engine cycles measured under steady state engine operation conditions. For the heat release calculations, the cylinder pressure at the inlet bottom dead center (BDC) was considered equal to the intake manifold pressure when the absolute in-cylinder pressure was calculated. Also, the top dead center (TDC) offset between the CAD measured by the encoder signal and the calculated in-cylinder volume was compensated for by setting the peak of the motored in-cylinder pressure at a fixed location (for a detailed explanation see [64].

An external compressor provided the oil-free dry air for the engine. The cooled, high-pressure exhaust gas recirculation (EGR) was introduced to the intake plenum for mixing with pressurized fresh air, and the mixture intake temperature (T_{in}) and pressure (P_{in}) were kept at ~ 26–28°C and ~1.85 bar, respectively. An adjustable EGR system, consisting of an EGR valve and an exhaust backpressure valve, provided a low level EGR, corresponding to 18% oxygen level in the intake mixture.

Engine lubricant and fuels

The engine was lubricated with synthetic low-ash motor oil (Shell Mysella S3 N40). The fuels used in the experiment were a fossil diesel (ultra-low sulfur Swedish MK1), and two sustainable diesel-like fuels: hydrotreated vegetable oil (HVO), and rapeseed methyl ester (RME). All test fuels consisted of a single kind of commercial fuel without any blending at the test facilities. Their physicochemical properties are shown in Table 2.

Table 2. Fuel specifications. [+]Provided by the manufacturer [65], *from [66].

	diesel*	**HVO[+]**	**RME***
CN	~53	>70	52
H/C	2	2.143	1.896
O/C	0.02	0	0.103
Q_{LHV}	43.15 MJ/kg	44.1 MJ/kg	37.3 MJ/kg
$(A/F)_S$	14.5	14.90	12.37

HVO has higher cetane number (CN) and energy density than fossil diesel, and compared to RME this difference is even more pronounced. RME is oxygenated fuel, which has a drawback of not as high lower heating value (Q_{LHV}) [67]. It is less stable, but on the other hand, it has highest density and viscosity and therefore does not need to be blended with lubricity additives. In terms of emissions, it has advantage of possibly lower CO, THC and PM emissions than other two fuels.

Exhaust aftertreatment system

The DOC used in this study was a metallic catalyst (Pt:Pd), operating at the engine exhaust temperature of 215 ± 6°C. This custom-made aftertreatment unit was dimensioned to fit the one-cylinder heavy-duty engine, so the exhaust residence time can be considered representative of the real engine operation.

Emissions analysis

Gaseous emissions

A Horiba emission system (MEXA-7500DEGR) analyzed the gaseous emission levels in the raw exhaust: THC, CO, NOx and O_2. The CO_2 concentration was measured both in the intake manifold and in the exhaust to provide the data for the calculation of the EGR level. The dry CO and CO_2 were measured with an infrared detector (IRD), whereas the wet NO and NO_x ($NO+NO_2$) were measured using a chemiluminescence detector (CLD). The wet total hydrocarbons (THC) was measured by a flame ionisation detector (FID). The CH_4 concentration is measured within the THC.

Particulate matter

A specific focus of this study is laid on chemical composition of organic fraction of PM from diesel combustion.

Dilution of exhaust gases

The sampling and dilution procedures of the exhaust gases from the engine are explained in detail in [21]. Exhaust gases for aerosol mass spectrometry (AMS) measurements were sampled continuously by extracting a small flow from the exhaust pipe which was diluted in three steps. The extracted flow was diluted in series by compressed HEPA-filtered and active carbon filtered air in a porous tube diluter with a dilution ratio (DR) of 12, followed by an ejector diluter with a DR of 9. The ejector diluter sustained the flow. A small residence tube (2.5 s) between the porous tube and ejector diluter allowed simulation of real-world conditions and a more representative particle nucleation [23]. This flow was continuously flowing through the potential aerosol mass (PAM) chamber and PAM bypass line. The AMS sampled after the third dilution stage that consisted of a second ejector diluter (DR 4-10) supplied with the same particle free compressed air. This third dilution pulled the flow through the PAM chamber and PAM bypass lines. The total dilution ratio was monitored by measuring the ratio of CO_2 in the exhaust and in the diluted aerosol. AMS data was corrected using average DRs calculated for each test.

Simulation of atmospheric aging

Secondary aerosol formation and changes in OA composition upon atmospheric aging were simulated with an oxidation flow reactor (OFR) [68]. The PAM-reactor uses UV light to initiate oxidative gas phase chemistry and simulates the equivalent of several days in the atmosphere during a few minutes' residence time in the OFR. The procedures applied in this campaign have been reported [21] and are only briefly repeated here. The PAM-reactor consists of a 13 L steel chamber containing two Hg lamps with peak intensities at 185 and 254 nm. In this study, only one of the lamps was used and operated at a reduced intensity. The flow rate through the PAM was controlled to 5–7 lpm, resulting in an average residence time in the chamber of 113–160 s. The same UV light intensity was employed in all the experiments. The incoming water vapor concentration was 0.37 ± 0.02 mol per m^3. CO (40 ppm) was added to the flow to allow calculation of the OH exposure in each experiment. The cumulative OH exposure was calculated from the reaction rate constant of CO and OH, and the CO concentrations. Due to variations in flow rate and OH suppression, the OH exposure varied somewhat between experiments. The OH exposure (molecules cm^{-3} s) corresponded to 4.8 ± 2.6 days if assuming an average OH concentration of 1.5×10^6 molecules cm^{-3}.

OA chemical composition by means of aerosol mass spectrometry

Aerosol mass spectrometry is an on-line technique that provides chemical characterization of OA without details on individual molecules, but has the advantage of fast acquisition times, providing near real-time data. Additionally, it provides bulk properties of the complete organic fraction in the PM. For example, the elemental composition given as O:C and H:C ratios.

The AMS and its quantification of OA have been described in detail in [69] and the references therein. In brief, AMS functions by focusing aerosol particles by means of an aerodynamic lens into a narrow beam. The beam impacts a heated surface at 600°C, the resulting vapors are ionized by means of electron impact, and then detected in a time of flight mass spectrometer. The software SQUIRREL 1.62 and PIKA 1.22 were used for data analysis and recommended praxis was followed with one exception. A HEPA filtered background air measurement was not available for assigning gas phase contribution to m/z 44 signal (CO_2^+) in these experiments. Gas phase CO_2^+ subtraction was instead carried out using external CO_2(g) measurements and assuming that the gas phase signal scales linearly with the measured sampling line mixing ratio in the range of 0–500 ppm.

Emission factors

Emission factors represent the mass of emitted pollutant per mass unit of burned fuel. The detailed description of the calculation method is given in [21]. In this study, the emission factors were normalized by the energy content of the fuel.

Experiments

Table 3 shows the summary of the conducted experiments. For all three fuels, engine-out emissions were analyzed, both fresh and after aging with the OFR. HVO exhaust was additionally studied after passing DOC aftertreatment, for both fresh and aged cases. Gaseous emissions downstream the DOC were measured only for diesel (marked with * in Table 3).

The following nomenclature was used: engine-out (EO) represents the fresh emissions without aging or aftertreatment, therefore fresh OA refers to the organic fraction of the PM measured EO (also EO OA). Organic fraction of the aged PM emissions is referred to as aged OA. Adding DOC to these initialisms means that emissions were measured after the aftertreatment system.

Table 3. Studied cases

	Diesel	HVO	RME
EO	fresh and aged	fresh and aged	fresh and aged
DOC	fresh and aged (*)	fresh and aged	X

Results and Discussion

Engine performance

The combustion efficiency (η_c) was high for all three fuels, above 99.2%. In order to compare combustion of fossil diesel, HVO and RME, in this steady-state test point, the rate of heat release (RoHR), in-cylinder pressure and injector current within a relevant window of crank angles were compared in Figure 2. The injector current represented by a black line is only an indication of the actual start of

injection (SOI) and end of injection (EOI). The EOI is clearly separated from the start of combustion defined as CA5, which gives a positive mixing period (MP). For all three fuels, the MP is positive in the range from 2.3 to 2.8 CAD, indicating that the combustion mode is LTC, PPC in particular [70], with very short combustion durations (10–11 CAD), which is one of the factors contributing to high efficiency of LTC. HVO has longer combustion duration than RME, leading to a longer duration of sooting flame, as reported previously [67].

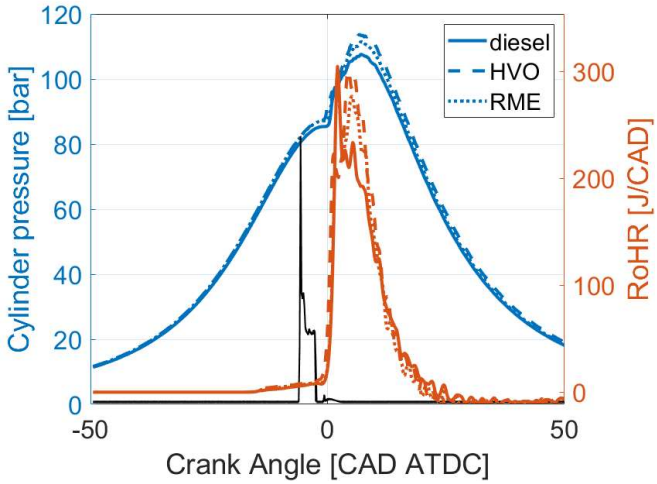

Figure 2. RoHR, in-cylinder pressure, and injector current for diesel, HVO and RME.

Emissions

Primary and secondary aerosol emissions

Figure 3 shows that emissions factors of HC and OA for HVO were slightly lower than those of diesel, around 20% and 30% respectively. At the same time, emission factors are around a factor of three lower for RME compared to diesel, for both HC and OA It can be seen in Figure 4 that aged OA emission factors are highest for diesel, about 2 times lower for HVO and about 8 times lower for RME. Similar to fresh OA, RME forms considerably less aged OA than the other fuels.

Aged OA corresponded to almost 9% of HC for diesel, if the values in Figure 3 and Figure 4 are compared. This indicates that a significant fraction of the gas phase HC is converted to particle phase OA in the atmosphere. These numbers for HVO and RME are near 5% and 3%, respectively. The lower fraction of HC converted to SOA for the renewable fuels may be due to differences in the chemical composition of the gas phase HC for the different fuels. It is well known that aromatic compounds and medium and long chain aliphatic compounds have a high SOA yield, while the SOA-yield of short chain aliphatics is much lower [71].

The OA enhancement upon aging, as measured with the AMS, was very high for all fuels when measured engine out. Almost 20 times more OA mass was detected when simulating ~5 days of atmospheric aging with the OFR, compared to the fresh emission for diesel. The OA enhancement was lowest for RME (~6). This is likely an upper estimate as a significant fraction of the fresh OA without DOC is present in nucleation mode particles that cannot be detected with the AMS (lower cut-point ~40 nm). Upon aging in the OFR the nucleation mode, particles grow considerably in size due to the condensation of SOA and thus a higher fraction of the mass can be detected by the AMS [21], biasing the OA enhancement high.

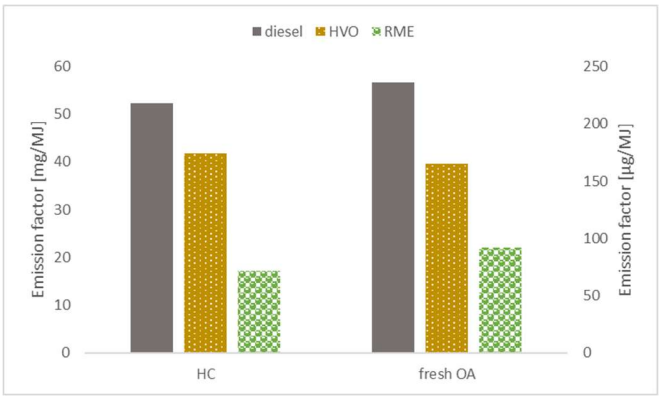

Figure 3. The emission factors of gaseous HC (left axis) and the OA fraction in PM (right axis) for all fuels measured engine-out.

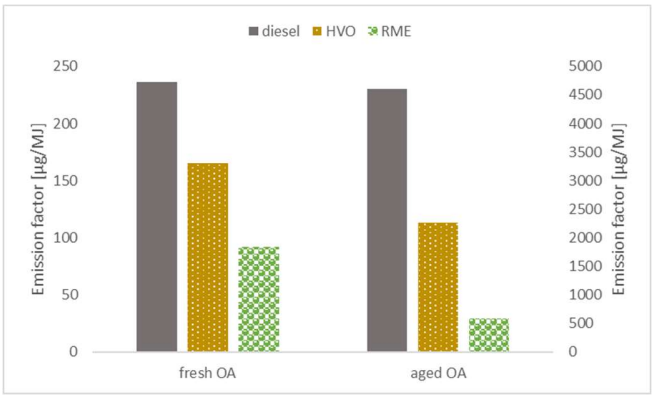

Figure 4. The emission factors of the fresh OA fraction in PM (left axis) and aged OA (right axis) for all fuels measured engine-out.

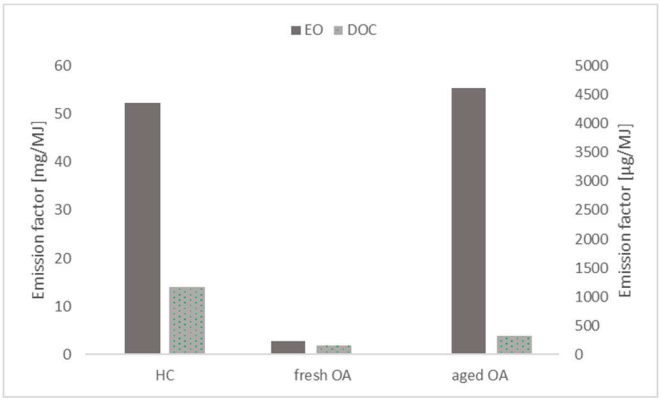

Figure 5. The emission factors of gaseous HC (left axis), the fresh OA fraction in PM (right axis) and aged OA (right axis) for diesel measured engine-out and after DOC.

SOA from traffic can be a major contributor to long range transported $PM_{2.5}$ in the atmosphere and thus our results for aged OA have implications for adverse health impacts of long range transported traffic air pollution.

The DOC strongly reduces HC, fresh OA and aged OA, see Figure 5. The strongest reduction is achieved for aged OA (a factor of more than 10). When an engine operates at low load, exhaust temperatures tend to be lower, which can result in DOC being less effective. In this experiment, however, the DOC was operated at around 215°C [21], which is not far from an appropriate temperature for high HC reduction.

The emission factors shown in this paper were previously calculated and presented in a different context in [21]. Uncertainties are not included in Figure 3–5. As an example, relative standard deviations

based on the time-series of HC measurements were 5–10% for all fuels.

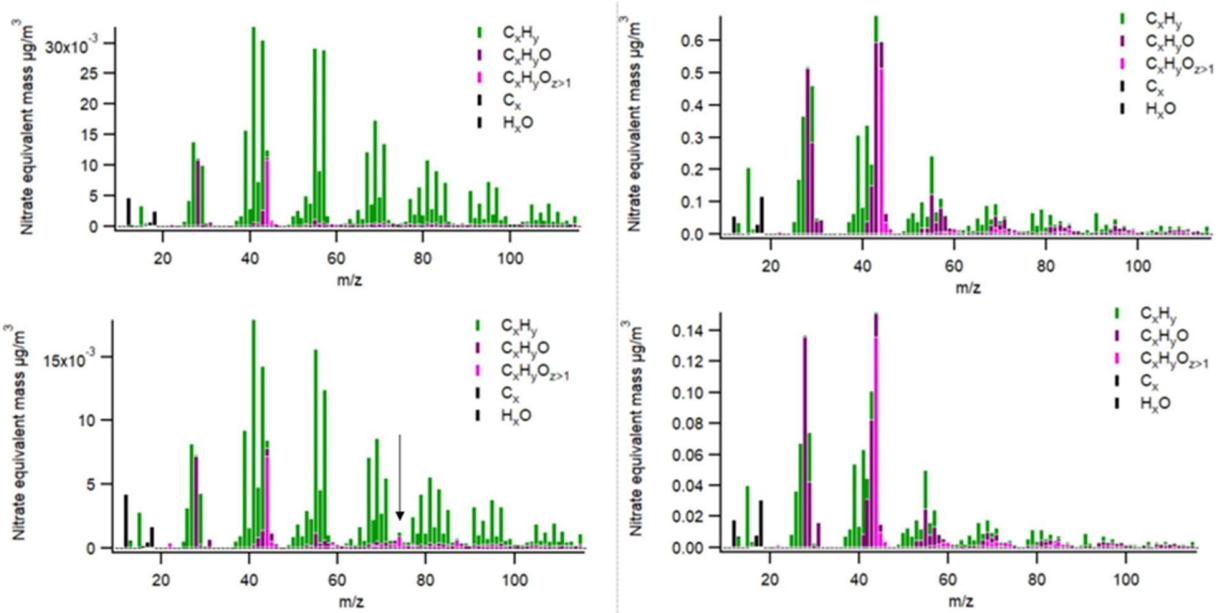

Figure 6. Organic aerosol mass spectra for fresh (left) and aged (right) exhaust: diesel (top) and RME (bottom). The vertical black arrow in the bottom left plot shows the identified RME marker (see text).

Composition of fresh and aged organic aerosol emissions

There was a striking similarity between the mass spectral signatures of OA from HVO and diesel fuels. The signature (see the left-hand side of Figure 6) strongly resembles hydrocarbon-like organic aerosol (HOA) mass spectra extracted from ambient datasets by e.g. [72] traffic organic aerosol near roadside. The abundance of lubrication oil in the particles may explain the similarities between fuels, and with ambient data.

There were also strong similarities in the OA mass spectra between diesel and RME. However, there is a clear marker for RME exhaust at m/z 74 ($C_3H_6O_2^+$), having a tenfold intensity increase of the ion for RME fuel compared to HVO and diesel, see the vertical black arrow in Figure 6. This fragment likely originates from the ester group in the original FAME molecules. It is a rather small signal as shown in Figure 6, so utilizing the marker in ambient data may be challenging. Additionally, the CO_2^+ (m/z=44) fragment was stronger for RME and hydrocarbon fragments with lower H:C ratio were slightly more abundant in RME compared to diesel (higher 41/43 and 55/57 ratio). When quantifying the elemental composition (Figure 7), the deviations for RME compared to diesel and HVO POA can be seen as a slightly higher O:C and a lower H:C ratio. Also, the results are consistent with fuel contributions for the RME case, as the fatty acid methyl esters in RME have a considerable oxygen content (~10%). The results correlate well with the previous findings in [73] where a HOA signature that represents POA from fossil fuel combustion with a low O:C ratio (0.06) was determined.

Another key finding was that the OA emissions of RME were almost 3 times lower than those for diesel and HVO. The lower OA emission factor of RME compared to diesel was also found in our previous studies in a similar engine at similar operating conditions [21][66].

The effect of DOC on OA chemical composition was evaluated for HVO. For both fresh and aged exhaust, DOC increases the average carbon oxidation state, by increasing O:C (for fresh: from 0.06 to 0.1; for aged, unchanged at 0.38) and decreasing H:C (fresh: 1.84 to 1.74, aged 1.47 to 1.44), see Figure 7.

As shown in Figure 7, the aged organic aerosol is much enriched in oxygen compared to the fresh exhaust. Organic aerosol is much more abundant in the exhaust after (artificial) aging, the particle mass concentration increases with time. This increase is due to gas phase oxidation of volatile organic compounds and hence the increased oxygen is to be expected.

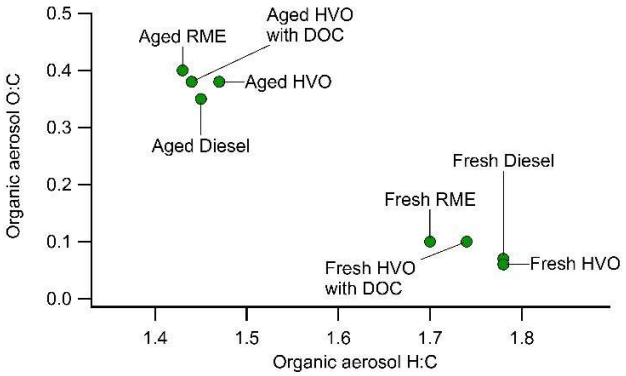

Figure 7. Overview of organic aerosol oxygen-to-carbon and hydrogen-to-carbon ratios for fresh and aged exhaust of diesel, RME and HVO.

Renewable diesel-like fuels, oxygenated RME and non-aromatic HVO, in OA source appointment behave somewhat differently. Fresh OA from HVO is very similar to that of fossil diesel, but its SOA has higher O:C value and lower H:C value.

Water uptake by an aerosol particle depends on the number of molecules and ions that it contributes to the aqueous phase. That is, it is favored by large size, low molar weight, high density, dissociation into ions and depends on the material being water-soluble. For these reasons the inorganic salts, as for example ammonium nitrate, show high hygroscopicity. For organic aerosol material, observations in [74] show an almost linear relation between the O:C ratio and the hygroscopicity [75]. The O:C ratio will therefore affect the water uptake, which is central in predicting the direct climate effect of aerosols. This is because it affects the ability of particles to act as cloud condensation nuclei (indirect aerosol effect on climate) [76]. This means that OA from RME emissions, with the highest O:C

values of both OA and SOA among the tested fuels, likely has tendency to absorb slightly more moisture form the atmosphere and behave differently than fossil diesel exhaust OA and SOA. In the atmosphere, the organic aerosol emitted from combustion of the different fuels will be mixed with a pre-existing aerosol and be subject to condensation of vapors which are in many cases water soluble. It is thus not straight forward to tell if the emissions will increase the number of CCN by increasing the particle number or if the effect is the opposite due to the total aerosol material being distributed over a higher number of particles that could be too small to act as cloud condensation nuclei at the actual atmospheric conditions.

Conclusion

The impact of the exhaust organic aerosol emissions from renewable diesel-like fuels, RME and HVO, in modern compression-ignition engines equipped with aftertreatment systems has recently become a focus of several studies. The impact of secondary organic aerosol emissions formed in the atmosphere is still largely unknown. Therefore, there is a need for characterization of the composition of the organic fraction of the emitted diesel PM.

In this study, the chemical composition of the organic aerosol emitted from a single-cylinder heavy-duty truck engine run on fossil diesel, HVO and RME, were studied by means of on-line aerosol mass spectrometry. Both fresh engine-out emissions and the impact on emissions by experimental simulation of atmospheric aging were investigated. Based on this work, the following conclusions can be made:

- The chemical structure of the primary organic aerosol for all three fuels are dominated by hydrocarbons with minor contribution of lightly oxidized molecules.
- RME both reduced the OA emissions and changed the composition with evidence for its specific fuel contributions in the mass spectra.
- OA emissions strongly increased for all three fuels when the emissions were aged in order to simulate secondary organic aerosol formation in the atmosphere. SOA formation was, however, substantially lower for RME compared to fossil diesel and HVO.
- The DOC strongly reduced primary organic emissions in both the gas (THC) and particle phase (OA). It was also effective in reducing SOA formation upon atmospheric aging.

These experiments give a fundamental understanding of differences between the fuels, and therefore the studied emission levels cannot be compared to the emission legislations.

In future studies, a design that may measure the emissions directly when the exhaust valves open would be preferable, instead of leading emissions through an exhaust pipe where certain transformations may occur. Fast sampling valve measurements with RME fuel would also give more specific answers to the questions that this paper tries to answer, as it was done for fossil diesel fuel previously in [45][77].

References

1. Gouw, J. de and Jimenez, J.L., “Organic aerosols in the earth’s atmosphere,” *Environ. Sci. Technol.* 43(20):7614–7618, 2009, doi:10.1021/es9006004.

2. Sun, J. and Ariya, P.A., “Atmospheric organic and bio-aerosols as cloud condensation nuclei (CCN): A review,” *Atmos. Environ.* 40(5):795–820, 2006, doi:10.1016/j.atmosenv.2005.05.052.

3. Kittelson, D.B., “Engines and nanoparticles: a review,” *J. Aerosol Sci.* 29(5):575–588, 1998, doi:10.1016/S0021-8502(97)10037-4.

4. Maricq, M.M., Chase, R.E., Xu, N., and Laing, P.M., “The Effects of the Catalytic Converter and Fuel Sulfur Level on Motor Vehicle Particulate Matter Emissions: Light Duty Diesel Vehicles,” *Environ. Sci. Technol.* 36(2):283–289, 2002, doi:10.1021/es010962l.

5. Rönkkö, T., Kuuluvainen, H., Karjalainen, P., Keskinen, J. et al., “Traffic is a major source of atmospheric nanocluster aerosol,” *Proceedings of the National Academy of Sciences* 114(29):7549–7554, 2017, doi:10.1073/pnas.1700830114.

6. Uhrner, U., Zallinger, M., Löwis, S. von, Vehkamäki, H. et al., “Volatile Nanoparticle Formation and Growth within a Diluting Diesel Car Exhaust,” *J. Air Waste Manage. Assoc.* 61(4):399–408, 2011, doi:10.3155/1047-3289.61.4.399.

7. Charron, A. and Harrison, R.M., “Primary particle formation from vehicle emissions during exhaust dilution in the roadside atmosphere,” *Atmos. Environ.* 37(29):4109–4119, 2003, doi:10.1016/S1352-2310(03)00510-7.

8. Casati, R., Scheer, V., Vogt, R., and Benter, T., “Measurement of nucleation and soot mode particle emission from a diesel passenger car in real world and laboratory in situ dilution,” *Atmos. Environ.* 41(10):2125–2135, 2007, doi:10.1016/j.atmosenv.2006.10.078.

9. Giechaskiel, B., Melas, A., Martini, G., Dilara, P. et al., “Revisiting Total Particle Number Measurements for Vehicle Exhaust Regulations,” *Atmosphere* 13(2), 2022, doi:10.3390/atmos13020155.

10. Rönkkö, T. and Timonen, H., “Overview of Sources and Characteristics of Nanoparticles in Urban Traffic-Influenced Areas,” *J. Alzheimer’s Dis.* 72:15–28, 2019, doi:10.3233/JAD-190170.

11. Kittelson, D.B., Watts, W.F., Johnson, J.P., Rowntree, C. et al., “On-road evaluation of two Diesel exhaust aftertreatment devices,” *J. Aerosol Sci.* 37(9):1140–1151, 2006, doi:10.1016/j.jaerosci.2005.11.003.

12. McMurry, P.H. and Friedlander, S.K., “New particle formation in the presence of an aerosol,” *Atmos. Environ. (1967)* 13(12):1635–1651, 1979, doi:10.1016/0004-6981(79)90322-6.

13. Morawska, L., Ristovski, Z., Jayaratne, E.R., Keogh, D.U. et al., “Ambient nano and ultrafine particles from motor vehicle emissions: Characteristics, ambient processing and implications on human exposure,” *Atmos. Environ.* 42(35):8113–8138, 2008, doi:10.1016/j.atmosenv.2008.07.050.

14. Murphy, D.M., Cziczo, D.J., Froyd, K.D., Hudson, P.K. et al., “Single-particle mass spectrometry of tropospheric aerosol particles,” *J. Geophys. Res. Atmos.* 111(D23), 2006, doi:10.1029/2006JD007340.

15. Zhang, Q., Jimenez, J.L., Canagaratna, M.R., Allan, J.D. et al., "Ubiquity and dominance of oxygenated species in organic aerosols in anthropogenically-influenced Northern Hemisphere midlatitudes," *Geophys. Res. Lett.* 34(13), 2007, doi:10.1029/2007GL029979.

16. Roth, P., Yang, J., Peng, W., Cocker, D.R. et al., "Intermediate and high ethanol blends reduce secondary organic aerosol formation from gasoline direct injection vehicles," *Atmos. Environ.* 220:117064, 2020, doi:10.1016/j.atmosenv.2019.117064.

17. Karjalainen, P., Timonen, H., Saukko, E., Kuuluvainen, H. et al., "Time-resolved characterization of primary particle emissions and secondary particle formation from a modern gasoline passenger car," *Atmos. Chem. Phys.* 16(13):8559–8570, 2016, doi:10.5194/acp-16-8559-2016.

18. Hallquist, M., Wenger, J.C., Baltensperger, U., Rudich, Y. et al., "The formation, properties and impact of secondary organic aerosol: current and emerging issues," *Atmos. Chem. Phys.* 9(14):5155–5236, 2009, doi:10.5194/acp-9-5155-2009.

19. Zhu, Q., Huang, X.-F., Cao, L.-M., Wei, L.-T. et al., "Improved source apportionment of organic aerosols in complex urban air pollution using the multilinear engine (ME-2)," *Atmos. Meas. Tech.* 11(2):1049–1060, 2018, doi:10.5194/amt-11-1049-2018.

20. Zhang, H. and Ying, Q., "Secondary organic aerosol from polycyclic aromatic hydrocarbons in Southeast Texas," *Atmos. Environ.* 55:279–287, 2012, doi:10.1016/j.atmosenv.2012.03.043.

21. Gren, L., Malmborg, V.B., Falk, J., Markula, L. et al., "Effects of renewable fuel and exhaust aftertreatment on primary and secondary emissions from a modern heavy-duty diesel engine," *J. Aerosol Sci.* 156, 2021, doi:10.1016/j.jaerosci.2021.105781.

22. Timonen, H., Karjalainen, P., Saukko, E., Saarikoski, S. et al., "Influence of fuel ethanol content on primary emissions and secondary aerosol formation potential for a modern flex-fuel gasoline vehicle," *Atmos. Chem. Phys.* 17(8):5311–5329, 2017, doi:10.5194/acp-17-5311-2017.

23. Karjalainen, P., Rönkkö, T., Simonen, P., Ntziachristos, L. et al., "Strategies To Diminish the Emissions of Particles and Secondary Aerosol Formation from Diesel Engines," *Environ. Sci. Technol.* 53(17):10408–10416, 2019, doi:10.1021/acs.est.9b04073.

24. Karavalakis, G., Durbin, T.D., Yang, J., Ventura, L. et al., "Fuel Effects on PM Emissions from Different Vehicle/Engine Configurations: A Literature Review," SAE Technical Paper 2018-01-0349, 2018, doi:10.4271/2018-01-0349.

25. Yang, J., Roth, P., Zhu, H., Durbin, T.D. et al., "Impacts of gasoline aromatic and ethanol levels on the emissions from GDI vehicles: Part 2. Influence on particulate matter, black carbon, and nanoparticle emissions," *Fuel* 252:812–820, 2019, doi:10.1016/j.fuel.2019.04.144.

26. Muñoz, M., Heeb, N. v, Haag, R., Honegger, P. et al., "Bioethanol Blending Reduces Nanoparticle, PAH, and Alkyl- and Nitro-PAH Emissions and the Genotoxic Potential of Exhaust from a Gasoline Direct Injection Flex-Fuel Vehicle," *Environ. Sci. Technol.* 50(21):11853–11861, 2016, doi:10.1021/acs.est.6b02606.

27. Distaso, E., Amirante, R., Calò, G., Palma, P. de et al., "Evolution of Soot Particle Number, Mass and Size Distribution along the Exhaust Line of a Heavy-Duty Engine Fueled with Compressed Natural Gas," *Energies* 13(15), 2020, doi:10.3390/en13153993.

28. Canagaratna, M.R., Jayne, J.T., Ghertner, D.A., Herndon, S. et al., "Chase Studies of Particulate Emissions from in-use New York City Vehicles," *Aerosol Sci. Technol.* 38(6):555–573, 2004, doi:10.1080/02786820490465504.

29. Carbone, S., Timonen, H.J., Rostedt, A., Happonen, M. et al., "Distinguishing fuel and lubricating oil combustion products in diesel engine exhaust particles," *Aerosol Sci. Technol.* 53(5):594–607, 2019, doi:10.1080/02786826.2019.1584389.

30. Breton, M. le, Psichoudaki, M., Hallquist, M., Watne, Å.K. et al., "Application of a FIGAERO ToF CIMS for on-line characterization of real-world fresh and aged particle emissions from buses," *Aerosol Sci. Technol.* 53(3):244–259, 2019, doi:10.1080/02786826.2019.1566592.

31. Tomasi, C., Fuzzi, S., and Kokhanovsky, A., eds., "Atmospheric Aerosols: Life Cycles and Effects on Air Quality and Climate," (Berlin, Wiley-VCH, 2017), ISBN 978-3-527-33645-6.

32. Volkamer, R., Jimenez, J.L., San Martini, F., Dzepina, K. et al., "Secondary organic aerosol formation from anthropogenic air pollution: Rapid and higher than expected," *Geophys. Res. Lett.* 33(17), 2006, doi:10.1029/2006GL026899.

33. Lanz, V.A., Alfarra, M.R., Baltensperger, U., Buchmann, B. et al., "Source apportionment of submicron organic aerosols at an urban site by factor analytical modelling of aerosol mass spectra," *Atmos. Chem. Phys.* 7(6):1503–1522, 2007, doi:10.5194/acp-7-1503-2007.

34. Nordin, E.Z., Eriksson, A.C., Roldin, P., Nilsson, P.T. et al., "Secondary organic aerosol formation from idling gasoline passenger vehicle emissions investigated in a smog chamber," *Atmos. Chem. Phys.* 13(12):6101–6116, 2013, doi:10.5194/acp-13-6101-2013.

35. Ye, J., Rooy, P. van, Adam, C.H., Jeong, C.-H. et al., "Predicting Secondary Organic Aerosol Enhancement in the Presence of Atmospherically Relevant Organic Particles," *ACS Earth Space Chem.* 2(10):1035–1046, 2018, doi:10.1021/acsearthspacechem.8b00093.

36. Gorkowski, K., Donahue, N.M., and Sullivan, R.C., "Aerosol Optical Tweezers Constrain the Morphology Evolution of Liquid-Liquid Phase-Separated Atmospheric Particles," *Chem.* 6(1):204–220, 2020, doi:10.1016/j.chempr.2019.10.018.

37. Schum, S.K., Zhang, B., Dzepina, K., Fialho, P. et al., "Molecular and physical characteristics of aerosol at a remote free troposphere site: Implications for atmospheric

aging," *Atmos. Chem. Phys.* 18(19):14017 – 14036, 2018, doi:10.5194/acp-18-14017-2018.

38. Gorkowski, K., Preston, T.C., and Zuend, A., "Relative-humidity-dependent organic aerosol thermodynamics via an efficient reduced-complexity model," *Atmos. Chem. Phys.* 19(21):13383–13407, 2019, doi:10.5194/acp-19-13383-2019.

39. Mahrt, F., Newman, E., Huang, Y., Ammann, M. et al., "Phase Behavior of Hydrocarbon-like Primary Organic Aerosol and Secondary Organic Aerosol Proxies Based on Their Elemental Oxygen-to-Carbon Ratio," *Environ. Sci. Technol.* 55(18):12202–12214, 2021, doi:10.1021/acs.est.1c02697.

40. Heyder, J., Gebhart, J., Rudolf, G., Schiller, C.F. et al., "Deposition of particles in the human respiratory tract in the size range 0.005–15 μm," *J. Aerosol Sci.* 17(5):811–825, 1986, doi:10.1016/0021-8502(86)90035-2.

41. Borm, P.J.A., Schins, R.P.F., and Albrecht, C., "Inhaled particles and lung cancer, part B: Paradigms and risk assessment," *Int. J. Cancer* 110(1):3–14, 2004, doi:10.1002/ijc.20064.

42. Ostiguy, C., Soucy, B., Lapointe, G., Woods, C. et al., "Health Effects of Nanoparticles, Second Edition," (Québec, IRSST, 2006), ISBN: 978-2-89631-320-4.

43. McKinsey & Company, "McKinsey Energy Insights Executive Summary: Global Energy Perspective 2022," https://www.mckinsey.com/industries/oil-and-gas/our-insights/global-energy-perspective-2022, accessed Aug. 2022.

44. Malmborg, V.B., Eriksson, A.C., Shen, M., Nilsson, P. et al., "Evolution of In-Cylinder Diesel Engine Soot and Emission Characteristics Investigated with Online Aerosol Mass Spectrometry," *Environ. Sci. Technol.* 51(3):1876–1885, 2017, doi:10.1021/acs.est.6b03391.

45. The European Commission, "Renewable Energy Directive (REDII)," 2018.

46. Lapuerta, M., Armas, O., and Rodríguez-Fernández, J., "Effect of biodiesel fuels on diesel engine emissions," *Prog. Energy Combust. Sci.* 34(2):198–223, 2008, doi:10.1016/j.pecs.2007.07.001.

47. Sun, J., Caton, J.A., and Jacobs, T.J., Oxides of nitrogen emissions from biodiesel-fuelled diesel engines, *Prog. Energy Combust. Sci.* 36(6):677–695, 2010, doi:10.1016/j.pecs.2010.02.004.

48. Karavalakis, G., Johnson, K.C., Hajbabaei, M., and Durbin, T.D., "Application of low-level biodiesel blends on heavy-duty (diesel) engines: Feedstock implications on NOx and particulate emissions," *Fuel* 181:259–268, 2016, doi:10.1016/j.fuel.2016.05.001.

49. Kim, D., Kim, S., Oh, S., and No, S.-Y., "Engine performance and emission characteristics of hydrotreated vegetable oil in light duty diesel engines," *Fuel* 125:36–43, 2014, doi:10.1016/j.fuel.2014.01.089.

50. Aatola, H., Larmi, M., Sarjovaara, T., and Mikkonen, S., "Hydrotreated Vegetable Oil (HVO) as a Renewable Diesel Fuel: Trade-off between NOx, Particulate Emission, and Fuel Consumption of a Heavy Duty Engine," *SAE Int. J. Engines* 1(1):1251–1262, 2009, doi:10.4271/2008-01-2500.

51. Kuronen, M., Mikkonen, S., Aakko, P., and Murtonen, T., "Hydrotreated Vegetable Oil as Fuel for Heavy Duty Diesel Engines," SAE Technical Paper 2007-01-4031, 2007, doi:10.4271/2007-01-4031.

52. Jacob, A., Ashok, B., Alagumalai, A., Chyuan, O.H. et al., "Critical review on third generation micro algae biodiesel production and its feasibility as future bioenergy for IC engine applications," *Energy Convers. Manag.* 228, 2021, doi:10.1016/j.enconman.2020.113655.

53. Lü, J., Sheahan, C., and Fu, P., "Metabolic engineering of algae for fourth generation biofuels production," *Energy Environ. Sci.* 4(7):2451–2466, 2011, doi:10.1039/C0EE00593B.

54. Giakoumis, E.G., Rakopoulos, C.D., Dimaratos, A.M., and Rakopoulos, D.C., "Exhaust emissions of diesel engines operating under transient conditions with biodiesel fuel blends," *Prog. Energy Combust. Sci.* 38(5):691–715, 2012, doi:10.1016/j.pecs.2012.05.002.

55. McCaffery, C., Karavalakis, G., Durbin, T., Jung, H. et al., "Engine-Out Emissions Characteristics of a Light Duty Vehicle Operating on a Hydrogenated Vegetable Oil Renewable Diesel," SAE Technical Paper 2020-01-0337, 2020, doi:10.4271/2020-01-0337.

56. Savic, N., Rahman, M.M., Miljevic, B., Saathoff, H. et al., "Influence of biodiesel fuel composition on the morphology and microstructure of particles emitted from diesel engines," *Carbon* 104:179–189, 2016, doi:10.1016/j.carbon.2016.03.061.

57. Xu, H., Ou, L., Li, Y., Hawkins, T.R. et al., "Life Cycle Greenhouse Gas Emissions of Biodiesel and Renewable Diesel Production in the United States," *Environ. Sci. Technol.* 56(12):7512–7521, 2022, doi:10.1021/acs.est.2c00289.

58. Reşitoğlu, İ.A., Altinişik, K., and Keskin, A., "The pollutant emissions from diesel-engine vehicles and exhaust aftertreatment systems," *Clean Technol. Environ. Policy* 17(1):15–27, 2015, doi:10.1007/s10098-014-0793-9.

59. Liu, Z.G., Eckerle, W.A., and Ottinger, N.A., "Gas-phase and semivolatile organic emissions from a modern nonroad diesel engine equipped with advanced aftertreatment," *J. Air Waste Manage. Assoc.* 68(12):1333–1345, 2018, doi:10.1080/10962247.2018.1505676.

60. Zeraati-Rezaei, S., Alam, M.S., Xu, H., Beddows, D.C. et al., "Size-resolved physico-chemical characterization of diesel exhaust particles and efficiency of exhaust aftertreatment," *Atmos. Environ.* 222:117021, 2020, doi:10.1016/j.atmosenv.2019.117021.

61. Novakovic, M., Tuner, M., Garcia, A., and Verhelst, S., "An Experimental Investigation of Directly Injected E85 Fuel in a Heavy-Duty Compression Ignition Engine," SAE

Technical Paper 2022-01-1050, 2022, doi:10.4271/2022-01-1050.

62. Aziz, A. bin, "High Octane Number Fuels in Advanced Combustion Modes for Sustainable Transportation," Ph.D. thesis, Lund University, 2020.

63. Tunestål, P., "TDC Offset Estimation from Motored Cylinder Pressure Data based on Heat Release Shaping," *Oil Gas Sci. Technol. – Revue d'IFP Energies Nouvelles* 66(4):705–716, 2011, doi:10.2516/ogst/2011144.

64. Neste Corporation, "Neste renewable diesel handbook," https://www.neste.com/sites/default/files/attachments/neste_renewable_diesel_handbook.pdf, accessed Oct. 2022.

65. Novakovic, M., Shamun, S., Malmborg, V.B., Kling, K.I. et al., "Regulated Emissions and Detailed Particle Characterisation for Diesel and RME Biodiesel Fuel Combustion with Varying EGR in a Heavy-Duty Engine," SAE Technical Paper 2019-01-2291, 2019, doi:10.4271/2019-01-2291.

66. Qiang, C., Hulkkonen, T., Kaario, O., and Larmi, M., "HVO, RME, and Diesel Fuel Combustion in an Optically Accessible Compression Ignition Engine," *Energy Fuels* 33(3):2489–2501, 2019, doi:10.1021/acs.energyfuels.8b03822.

67. Kang, E., Root, M.J., Toohey, D.W., and Brune, W.H., "Introducing the concept of Potential Aerosol Mass (PAM)," *Atmos. Chem. Phys.* 7(22):5727–5744, 2007, doi:10.5194/acp-7-5727-2007.

68. Canagaratna, M.R., Jayne, J.T., Jimenez, J.L., Allan, J.D. et al., "Chemical and microphysical characterization of ambient aerosols with the aerodyne aerosol mass spectrometer," *Mass Spectrom. Rev.* 26(2):185–222, 2007, doi:10.1002/mas.20115.

69. Manente, V., Johansson, B., and Cannella, W., "Gasoline partially premixed combustion, the future of internal combustion engines?" *Int. J. Engine Res.* 12(3):194–208, 2011, doi:10.1177/1468087411402441.

70. Gentner, D.R., Jathar, S.H., Gordon, T.D., Bahreini, R. et al., "Review of Urban Secondary Organic Aerosol Formation from Gasoline and Diesel Motor Vehicle Emissions," *Environ. Sci. Technol.* 51(3):1074–1093, 2017, doi:10.1021/acs.est.6b04509.

71. Crippa, M., Decarlo, P.F., Slowik, J.G., Mohr, C. et al., "Wintertime aerosol chemical composition and source apportionment of the organic fraction in the metropolitan area of Paris," *Atmos. Chem. Phys.* 13(2):961–981, 2013, doi:10.5194/acp-13-961-2013.

72. Kroll, J.H., Donahue, N.M., Jimenez, J.L., Kessler, S.H. et al., "Carbon oxidation state as a metric for describing the chemistry of atmospheric organic aerosol," *Nat. Chem.* 3(2):133–139, 2011, doi:10.1038/nchem.948.

73. Jimenez, J.L., Canagaratna, M.R., Donahue, N.M., Prevot, A.S.H. et al., "Evolution of Organic Aerosols in the Atmosphere," *Science (1979)* 326(5959):1525–1529, 2009, doi:10.1126/science.1180353.

74. Petters, M.D. and Kreidenweis, S.M., "A single parameter representation of hygroscopic growth and cloud condensation nucleus activity," *Atmos. Chem. Phys.* 7(8):1961–1971, 2007, doi:10.5194/acp-7-1961-2007.

75. Tost, H. and Pringle, K.J., "Improvements of organic aerosol representations and their effects in large-scale atmospheric models," *Atmos. Chem. Phys.* 12(18):8687–8709, 2012, doi:10.5194/acp-12-8687-2012.

76. Shen, M., Malmborg, V., Gallo, Y., Waldheim, B.B.O. et al., "Analysis of Soot Particles in the Cylinder of a Heavy Duty Diesel Engine with High EGR," SAE Technical Paper 2015-24-2448, 2015, doi:10.4271/2015-24-2448.

Contact Information

Maja Novakovic
Division of combustion engines, Energy Sciences
Lund University, Sweden
Maja.Novakovic@energy.lth.se

Acknowledgments

This research was conducted within the KCFP Engine Research Center, supported by the Swedish Energy Agency grant number 22485-4, and the Swedish Research Council FORMAS (2016–00697), Sweden. We thank Vikram Singh, Kimmo Korhonen, John Falk, Thomas Bjerring Kristensen, and Lassi Markkula for technical assistance and supporting measurements during the campaign.

Definitions/Abbreviations

(A/F)s	stoichiometric air-fuel ratio
AMS	aerosol mass spectrometry
ATDC	after top dead center
BDC	bottom dead center
CA5	The crank angle at which 5% of the charge has been consumed, start of combustion.
CA50	Combustion phasing, the crank angle at which 50% of the charge has been consumed.
CAD	crank angle degrees
CCN	cloud condensation nuclei
CH_4	methane
CLD	chemiluminescence detector
CN	cetane number
CO	carbon monoxide

CO_2	carbon dioxide
DOC	diesel oxidation catalyst
DR	dilution ratio
EATS	exhaust aftertreatment system
EGR	exhaust gas recirculation
EO	engine-out
EOI	end of injection
FAME	fatty acid methyl ester
FID	flame ionization detector
GHG	greenhouse gas
HC	hydrocarbon
HD	heavy-duty
Hg	mercury
HOA	hydrocarbon-like organic aerosol
HVO	hydrotreated vegetable oil
hygroscopicity	ability to absorb moisture from the environment
ICE	internal combustion engine
IMEP	indicated mean effective pressure
IRD	infrared detector
LTC	low temperature combustion
MP	mixing period
NO	nitric oxide
NO_2	nitrogen dioxide
NOx	nitrogen oxides
OA	organic aerosol
PAH	polycyclic aromatic hydrocarbons
PAM	potential aerosol mass
Pd	palladium
PM	particulate matter
POA	primary organic aerosol
PPC	partially premixed combustion
Pt	platinum
Q_{LHF}	lower heating value
r_c	geometrical compression ratio
RME	rapeseed methyl ester
RoHR	rate of heat release
SOA	secondary organic aerosol
SOI	start of injection
TDC	top dead center
THC	total hydrocarbons
VOC	volatile organic compound
XPI	high-pressure injection
η_c	combustion efficiency